Microscopic Modeling of High Frequency Noise in SiGe HBTs

Mindaugas Ramonas * ‡, Paulius Sakalas † ‡, Christoph Jungemann *, Michael Schroter † §,
Wolfgang Kraus ¶, Artur Shimukovitch ‡
* EIT4, Bundeswehr University, 85577 Neubiberg, Germany, Email: ramonas@pfi.lt
† CEDIC, Dresden University of Technology, 01062 Dresden, Germany
‡ FRL, Semiconductor Physics Institute, 01108 Vilnius, Lithuania
§ ECE Dept., University of California, San Diego, USA
¶ Atmel Germany GmbH&, Theresienstrasse 2, 74072 Heilbronn, Germany

***Abstract*— The SIMS doping profile of SiGe heterojunction bipolar transistor is calibrated for best agreement of the hydrodynamic model results with the experiment. DC and small-signal data is used for the calibration. The terminal current noise calculations are performed using both hydrodynamic and drift-diffusion models with the calibrated doping profile. The calculation results are compared with the experimental values. Overall good agreement for the minimum noise figure, the noise resistance, and the optimum reflection coefficient is obtained. The difference between the hydrodynamic and drift-diffusion model results is analyzed using spectral intensities of the base and collector current fluctuations.**

I. Introduction

SiGe heterojunction bipolar transistors (HBTs) have successfully been introduced into RF market due to good high-frequency performance and compatibility with the existing silicon technology [1]. The noise performance is of high importance for RF applications, thus the knowledge of the noise figure for SiGe HBTs is essential. The experimental measurements of the noise figure in contrary to the DC and small signal measurements are complicated, time-consuming and hardly suitable for industrial applications.

Simple SPICE-Gummel-Poon compact models are often used to calculate the HBT noise figure using measured Y parameters [2]. Physical noise sources are represented by the shot noise due to the particles overcoming potential barriers and the thermal noise due to resistances. For the correct noise modeling at higher frequencies additional parameters have to be introduced, with ongoing discussion on the physical meaning and the experimental evaluation techniques [3]–[5]. Hydrodynamic (HD) and drift-diffusion (DD) models are based on carrier transport equations. Device doping profile and material constants are used as an input, and noise figure of the device can be calculated without any additional external parameters.

Both, terminal currents and small signal behavior of the transistor are very sensitive to the details of the doping profile. Large deviations in currents and Y parameters can be obtained even within the accuracy of measured SIMS doping profile. In this work the HD simulator is used to calibrate transistor doping profile within the accuracy of SIMS measurements. The good agreement between the modeling and the experimental values for DC and small signal results is used as a calibration criteria. Calculations of the noise figure for the SiGe HBT with the calibrated profile are performed with the HD and DD models. The calculation results are compared with the experimental values.

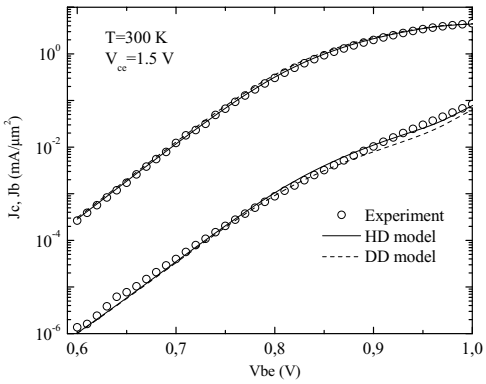

Fig. 1. Collector (J_c) and base (J_b) current densities: solid lines hydrodynamic and dashed lines drift-diffusion model results. Open circles represent the experimental values.

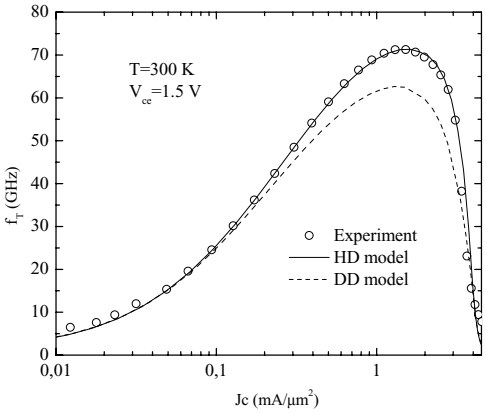

Fig. 2. Cutoff frequency (f_T): solid lines hydrodynamic, dashed lines drift-diffusion model results. Open circles represent the experimental values.

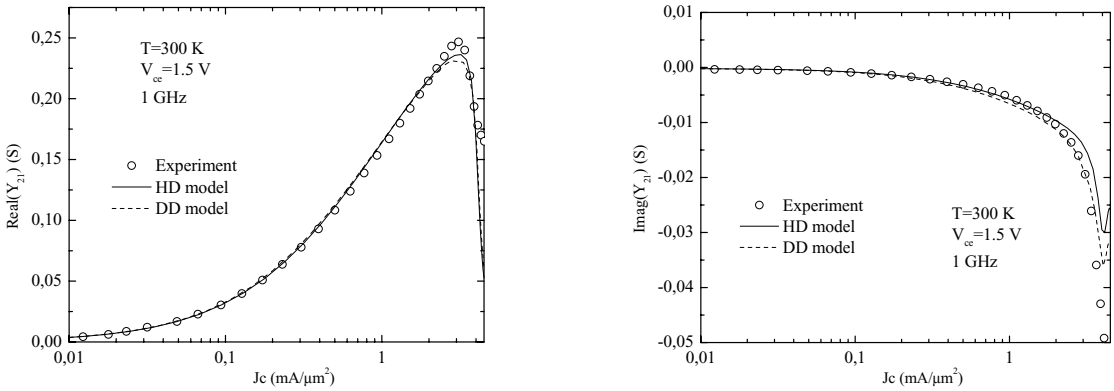

Fig. 3. Real (a) and imaginary part (b) of Y_{21}: solid lines hydrodynamic and dashed lines drift-diffusion results. Open circles represent the experimental values.

II. Doping profile calibration

Both, HD and DD calculations are performed using simulator Galene III [6]. The silicon and SiGe transport and noise parameters used in the simulator are generated with the Monte Carlo simulator Elwomis [7]. The band gap narrowing due to both, heavy doping and germanium content is included. Due to strong power dissipation the temperature of the transistor is higher than ambient temperature and self-heating effect has to be included in the simulations at high base-emitter bias ($V_{\rm be}$). Transistor self-heating effect is included in a self-consistent way. The temperature of the device is calculated iteratively at each bias point, using the thermal resistance and calculated terminal currents.

A SiGe NPN HBT with a CBEBC symmetric configuration and an emitter window 0.5*20.3 $\mu{\rm m}^2$ is investigated [8]. The cutoff frequency ($f_{\rm T}$) of the transistor is 70 GHz. All the calculations are performed for common emitter configuration at room temperature and 1.5 V collector-emitter bias. The doping profile of the modeled structure is calibrated using the DC and small signal experimental values.

An analytic profile derived from the SIMS measurements is used as the starting profile. Parameters Y_{11} and Y_{21} define transistor small signal behavior in forward active mode. The calibration function is constructed using the collector current, $f_{\rm T}$, and real and imaginary parts of the Y_{21} (1 GHz and 10 GHz frequencies) at five base-emitter bias points. Values at the low injection ($V_{\rm be}$= 0.7 V, 0.76 V), near the maximum of $f_{\rm T}$ ($V_{\rm be}$=0.85 V) and at the high injection ($V_{\rm be}$=0.94 V and 0.97 V) are used. Standard parameter for transistor small signal characterization $f_{\rm T}$ contains both Y_{11} and Y_{21} and is used instead of Y_{11} in the calibration function. Asynchronous Parallel Pattern Search algorithm is used to find the minimum of the calibration function [9]. The code can be run in parallel on a cluster of computers, greatly reducing the total calibration time. Constrains are imposed on the parameters of analytic doping profile to avoid large deviations from the SIMS profile.

The Gummel plot for the calibrated profile is shown in Fig. 1. The results of the DD and HD models are presented together with the experimental results. The results for the calibrated profile are in good agreement with the measured values in the whole range of the investigated base-emitter bias. The transistor cutoff frequency dependence on the collector current is presented in Fig. 2. The HD model (Fig. 2, solid line) results are in excellent agreement with the experiment up to the high-injection currents. Due to the velocity overshoot in the base of the transistor, which is not captured by the DD model, it gives lower maximum cutoff frequency. Modeling results for the real and the imaginary part of collector-base admittance Y_{21} at 1 GHz (Fig. 3) and 10 GHz frequency fit well with the experimental values up to high currents (4 mA/$\mu{\rm m}^2$). Good agreement for $f_{\rm T}$ and Y_{21} shows that the HD model is capable to reproduce HBT small signal operation in the forward active mode. The calibrated doping profile is used to calculate the noise figure of the HBT.

III. Noise modeling

The HBT noise behavior is modeled at 1 GHz, 8 GHz, and 25 GHz frequency. The Langevin-type noise model, implemented in the Galene III simulator [10], is used for the modeling. The noise due to the electron and hole scattering in the conduction and valence bands and the noise due to Shockley-Read-Hall recombination is considered. 1/f-noise is important only at low frequencies and is excluded from our calculations. The modeling is performed for collector-emitter bias ($V_{\rm ce}$=1.5 V) considerably lower than collector-emitter breakdown voltage for the investigated transistors ($V_{\rm ceO}$=2.5 V) and breakdown, tunneling, and impact ionization processes are not included.

On-wafer DC, AC (frequency range 0.1-40 GHz) standard characteristics were measured with HP4241, HP8510C, using Agilent ICCAP 2006 software and Suss Microtech semiautomatic RF-probestation PA200 and Cascade "'infinity" 150m pitch probes. Noise parameters (NP) were measured in 1-25 GHz range with automated tuner system ATS MT993B from Maury Microwaves, using high matching tuners MT982E (VSWR:15:1). Matching tuner at the output port enabled an

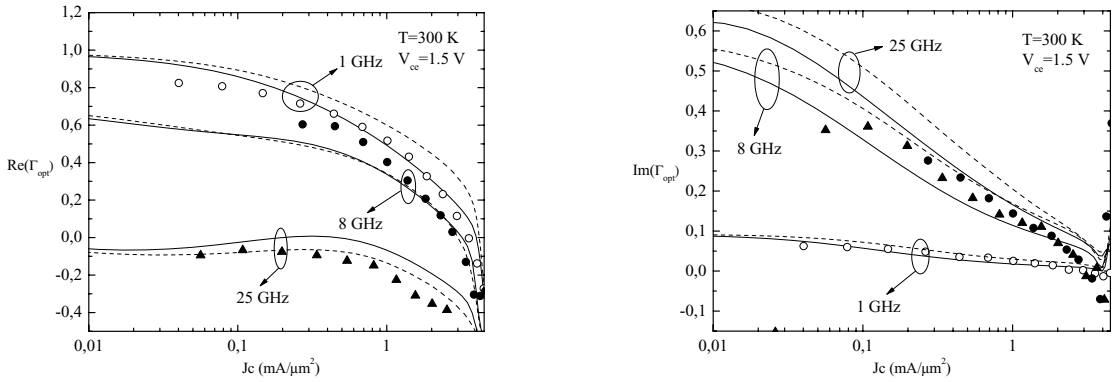

Fig. 4. Real part (a) and imaginary part (b) of the optimum reflection coefficient $\Gamma_{\rm opt}$: solid lines hydrodynamic, dashed lines drift-diffusion model results. Open circles, closed circles, and closed triangles represent the experimental values correspondingly at 1 GHz, 8 GHz and 25 GHz.

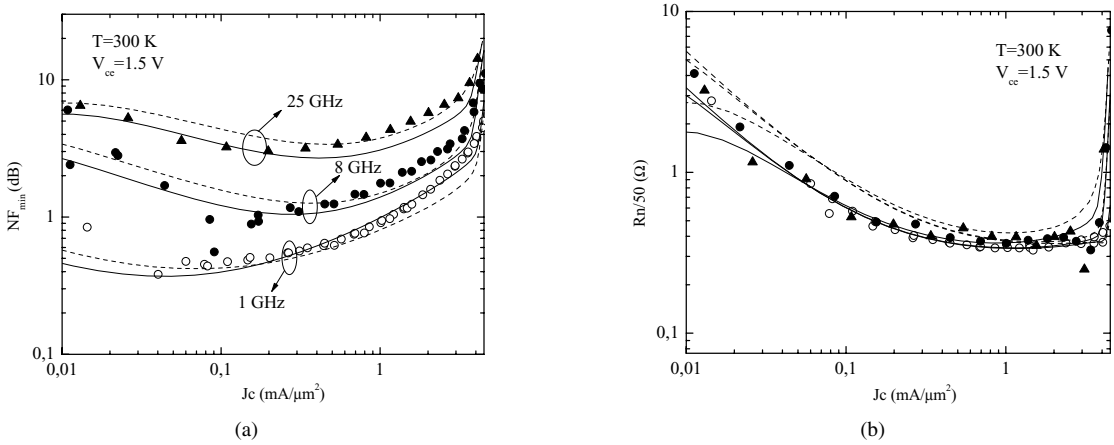

Fig. 5. Minimum noise figure ($\rm NF_{min}$) (a) and noise resistance ($\rm R_n$) (b): solid lines hydrodynamic, dashed lines drift-diffusion model results. Open circles, closed circles, and closed triangles represent the experimental values correspondingly at 1 GHz, 8 GHz and 25 GHz.

increase of the receiver sensitivity. Deembedding of pad parasitic network influence on NPs was performed with correlation matrix technique.

The results for optimum reflection coefficient, minimum noise figure and noise resistance calculated using HD (solid lines) and DD (dashed lines) models are shown together with the experimental values (open circles, closed circles, and closed triangles) in Fig. 4, Fig. 5(a), and Fig. 5(b). Overall good agreement with experimental results at 1 GHz, 8 GHz and 25 GHz frequencies is obtained for the HD model. The minimum noise figure calculated by the DD model is higher than the one obtained by the HD model for currents up to 0.2 mA/μm^2 for 1 GHz, 1 mA/μm^2 for 8 GHz, and in all range of investigated currents for 25 GHz frequency. On the other hand at 1 GHz and high currents DD gives lower values of minimum noise figure than HD model.

The reason of higher values for the noise figure at low currents in the DD model can be clarified by analyzing the spectral intensity of the collector current fluctuations. At low collector currents collector noise is mainly due to electrons overcoming emitter-base barrier and the spectral intensity obtained by the HD model (Fig. 6, solid lines) can be well described by the collector current shot noise $2q_eI_c$ (dotted line in Fig. 6). This is the approximation, usually used in simple SPICE-Gummel-Poon compact models [5]. At high currents collector current noise exceeds shot noise due to the increasing contribution of hole scattering [11]. The collector current noise obtained by the DD model is higher than shot noise even at low currents. This unphysical "supershot" noise [11] results in a higher noise figure at low currents. The frequency dependence of the spectral intensity of collector current fluctuations is weak (Fig. 6, black and gray lines) and higher $\rm NF_{min}$ values are obtained at 1 GHz, 8 GHz and 25 GHz.

Spectral intensity of the base current fluctuations for 1 GHz and 8 GHz frequencies is shown in the Fig. 7. At low currents base current noise for both frequencies is determined by thermal noise and transistor input capacitance. At 1 GHz and the currents exceeding 0.1 mA/μm^2 the main contribution to the base current noise comes from the holes overcoming base-emitter barrier, and noise can be well described by the base current shot noise (Fig. 7, gray lines). Since base current calculated using the DD model is lower than the one obtained

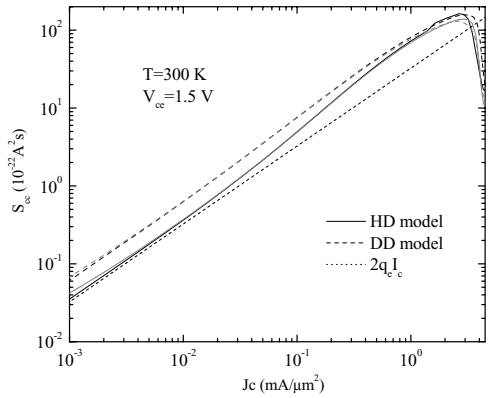

Fig. 6. Spectral intensity of the collector current fluctuations: solid lines hydrodynamic model and dashed lines drift-diffusion model results (black for 1 GHz and gray for 8 GHz). Dotted line– shot noise due to the collector current ($2q_{\mathrm{e}}I_{\mathrm{c}}$).

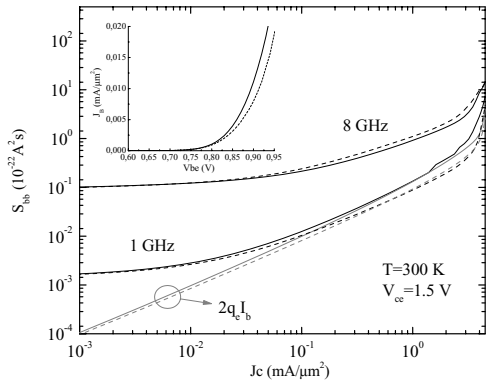

Fig. 7. Spectral intensity of the base current fluctuations: solid lines hydrodynamic model and dashed lines drift-diffusion model results. Gray color represents the shot noise due to the base current ($2q_{\mathrm{e}}I_{\mathrm{b}}$). The base current is shown in the inset of the figure.

from the HD model (inset of Fig. 7), the shot noise and consequently overall base current noise is lower for the DD model (Fig. 7, dashed lines). Lower base current noise causes lower minimum noise figure for DD model at 1 GHz frequency and high collector current (Fig. 5(a), dashed line). At 8 GHz frequency the main contribution to the base current noise comes from the thermal noise, and spectral intensity of the base current fluctuations calculated from the DD model is higher than calculated from the HD model for all currents under consideration.

IV. Conclusions

The HBT doping profile is calibrated for the best agreement between the hydrodynamic simulation and the experimental results on DC and small signal parameters. Calibrated profile is used in the hydrodynamic and the drift-diffusion simulator to calculate the noise figure of the HBT. The calculation results are verified against the experimental values. Good agreement for the noise figure is obtained up to 25 GHz frequency and high injection without any additional parameter fitting.

Acknowledgment

The authors would like to thank Atmel GmbH Heilbronn for providing wafers and German Research Society (DFG) for financial support.

References

[1] J. Cressler (ed.), *The SiGe Handbook*, CRC Press, NY, 2005.
[2] S. P. Voinigescu, M. C. Maliepaard, J. L. Showell, G. E. Babcock, D. Marchesan, M. Schroter, P. Schvan, and D. L. Harame, "A Scalable High-Frequency Noise Model for Bipolar Transistors with Application to Optimal Transistor Sizing for Low-Noise Amplifier Design," *IEEE J. Solid-State Circuits*, vol. 32, pp. 1430-1439, 1997.
[3] M. Rudolph, R. Doerner, L. Klapproth, and P. Heymann, "An HBT Noise Model Valid Up to Transit Frequency," *IEEE Electron Device Lett.*, vol. 20, pp. 24-26, 1999.
[4] G. Niu, J. D. Cressler, S. Zhang, W. E. Ansley, C. S. Webster, and D. L. Harame, "A Unified Approach to RF and Microwave Noise Parameter Modeling in Bipolar Transistors," *IEEE Trans. Electron Devices*, vol. 48, pp. 2568-2574, 2001.
[5] C. Jungemann, B. Neinhüs, B. Meinerzhagen, and R. W. Dutton, "Investigation of Compact Models for RF Noise in SiGe HBTs by Hydrodynamic Device Simulation," *IEEE Trans. Electron Devices*, vol. 51, pp. 956-961, 2004.
[6] B. Neinhüs, S. Decker, P. Graf, F. M. Bufler, and B. Meinerzhagen, "Consistent Hydrodynamic and Monte-Carlo Simulation of SiGe HBTs Based on Table Models for the Relaxation Times," *VLSI Design*, vol. 8, pp. 387-391, 1998.
[7] C. Jungemann, S. Keith, and B. Meinerzhagen, "Full-band Monte Carlo device simulation of a Si/SiGe-HBT with a realistic Ge profile," *IEICE Trans. on Electronics*, vol. E83-C, pp. 1228-1234, 2000.
[8] http://www.atmel.com/products/SiGeBipolar.
[9] http://software.sandia.gov/appspack
[10] C. Jungemann, B. Neinhüs, and B. Meinerzhagen, "Hierarchical 2-D DD and HD Noise Simulations of Si and SiGe Devices–Part I: Theory," *IEEE Trans. Electron Devices*, vol. 49, pp. 1250-1257, 2002.
[11] C. Jungemann, B. Neinhüs, S. Decker, and B. Meinerzhagen, "Hierarchical 2-D DD and HD Noise Simulations of Si and SiGe Devices–Part II: Results," *IEEE Trans. Electron Devices*, vol. 49, pp. 1258-1264, 2002.